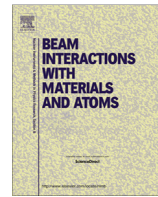




Contents lists available at ScienceDirect



## Comparative *ab initio* calculations of SrTiO<sub>3</sub>/BaTiO<sub>3</sub> and SrZrO<sub>3</sub>/PbZrO<sub>3</sub> (001) heterostructures

Sergei Piskunov\*, Roberts I. Eglitis

Institute of Solid State Physics, University of Latvia, 8 Kengaraga str., Riga LV-1063, Latvia

## ARTICLE INFO

## Article history:

Received 29 May 2015

Received in revised form 30 June 2015

Accepted 2 July 2015

Available online xxxx

## Keywords:

ABO<sub>3</sub> perovskites

(001) interfaces

Electronic structure

Hybrid HF-DFT B3PW calculations

## ABSTRACT

Using a B3PW hybrid exchange–correlation functional within the density functional theory (DFT) we calculated from the first principles the electronic structure of BaTiO<sub>3</sub>/SrTiO<sub>3</sub> and PbZrO<sub>3</sub>/SrZrO<sub>3</sub> (001) interfaces. The optical band gap of both BaTiO<sub>3</sub>/SrTiO<sub>3</sub> and PbZrO<sub>3</sub>/SrZrO<sub>3</sub> (001) interfaces depends mostly from BaO or TiO<sub>2</sub> and SrO or ZrO<sub>2</sub> termination of the upper layer, respectively. Based on the results of our calculations we predict increase of the Ti–O and Zr–O chemical bond covalency near the SrTiO<sub>3</sub>/BaTiO<sub>3</sub> and SrZrO<sub>3</sub>/PbZrO<sub>3</sub> (001) interfaces as compared to the BaTiO<sub>3</sub> and PbZrO<sub>3</sub> bulk.

© 2015 Elsevier B.V. All rights reserved.

## 1. Introduction

Modern science and industry allow the growth of superlattices and ultrathin films with atomic control. The exploration of complex oxide heterostructures is very promising field due to potential nanoscale device applications. The BaTiO<sub>3</sub>/SrTiO<sub>3</sub> and PbZrO<sub>3</sub>/SrZrO<sub>3</sub> (001) interfaces present an excellent possibility for developing novel materials with outstanding properties, as well as they are extremely important in studying the fundamental physics of ferroelectric materials. Despite the huge technological importance of SrTiO<sub>3</sub> (STO), BaTiO<sub>3</sub> (BTO), SrZrO<sub>3</sub> (SZO) and PbZrO<sub>3</sub> (PZO) perovskites, and numerous *ab initio* studies of their (001) surfaces, [1–13], it is hard to understand, why only a small amount of *ab initio* and experimental studies exist dealing with BTO/STO (001) interface [14–19]. There are no experimental studies available, and only single *ab initio* calculation [20] exist dealing with PZO/SZO (001) interface.

In our paper, we present an overview of charge density redistribution in both stoichiometric and non-stoichiometric atomically sharp interfaces consisting of BTO (001) and PZO (001) thin films having thickness from 1 to 10 monolayers (0.5–5.0 unit cells) and deposited atop of TiO<sub>2</sub>-terminated STO (001) and ZrO<sub>2</sub>-terminated SZO (001) substrate. The first principles methods used for simulations are based on the DFT theory accompanied with hybrid exchange–correlation functional. The B3PW functional [21] used in the current study contains a “hybrid” of the DFT

exchange and correlation functionals with exact non-local Hartree–Fock (HF) exchange. Standard BTO, STO, PZO and SZO low index (001) surfaces have been carefully studied by us already previously [2,1,22,23,7,8,12,6,13].

The present contribution is structured as follows. Section 2 describes the calculation details. The main part of the paper is described in Section 3. The Section 3 presents electronic charge distribution and changes in band structure for PZO/SZO and BTO/STO (001) interfaces and discusses their relation to the experimental data and previous *ab initio* calculations. Our conclusions are summarized in Section 4.

## 2. Computational details

In the present study BTO/STO (001) and PZO/SZO (001) interfaces are simulated by means of the linear combination of atomic orbitals (LCAO) approach within the framework of hybrid density functional theory. With aim to perform hybrid LCAO calculations, the periodic CRYSTAL code [24], which employs Gaussian-type functions centered on atomic nuclei as the basis sets (BSs) was used. The following BSs: For Ba, Sr, Ti, Zr and O in the form of 311d1G, 411d311G, 311d31G and 8–411d1G, respectively, from Refs. [25,24] were used. The inner core electrons of Ba, Sr, Zr and Ti are described by small-core Hay–Wadt effective pseudopotentials [26].

We use the well-known hybrid B3PW exchange–correlation functional [21] which accurately describes the basic bulk and surface properties of a number of ABO<sub>3</sub> materials [25,23,27]. The

\* Corresponding author.

E-mail addresses: [piskunov@lu.lv](mailto:piskunov@lu.lv) (S. Piskunov), [rieglitis@gmail.com](mailto:rieglitis@gmail.com) (R.I. Eglitis).

band gaps obtained by means of hybrid B3PW computation scheme are in better agreement with experimentally observed results than pure DFT calculations [25]. Bond populations and effective charges on atoms have been calculated according to the Mulliken population analysis [28]. In our calculations the reciprocal space integration was performed by sampling the Brillouin zone with the  $8 \times 8 \times 1$  Pack–Monkhorst mesh [29] for all explored interface structures.

Taking into account that STO and SZO substrates at room temperature possesses perfect cubic structure, in our study we calculate BTO, PZO, SZO and STO in their high symmetry cubic  $Pm\bar{3}m$  phase. Table 1 contains calculated bulk properties for all four perovskites. Surface structures were modeled using a single slab model. To maximize the use of symmetry our slabs are symmetrically terminated. STO (001) and SZO (001) substrates contain 11 alternating ( $\text{SrO}$ ) and ( $\text{ZrTiO}_2$ ) atomic monolayers, while from 1 to 10 alternating ( $\text{BaO}$ ) or ( $\text{PbO}$ ) and ( $\text{TiO}_2$ ) or ( $\text{ZrO}_2$ ) atomic monolayers were used for BTO (001) and PZO (001) films of the BTO/STO (001) and PZO/SZO (001) interfaces, respectively (Fig. 1). Coordinates of all atoms in the BTO/STO (001) and PZO/SZO (001) interfaces were set free to relax. Due to symmetry constrains atomic displacements are allowed only along z-axis. Taking into account that the large mismatch of  $\sim 2.5\%$  between BTO and STO, as well as small one of  $\sim 0.2\%$  between PZO and SZO lattice constants arises during BTO or PZO epitaxial growth, in our simulations we have allowed relaxation of their joint lattice constant to minimize the strain effect.

### 3. Results of numerical calculations and discussion

Simulations of the atomic and electronic properties of the BTO/STO and PZO/SZO (001) interfaces were performed using the symmetrically terminated slab model. The STO and SZO (001) substrates consisted of 11 atomic monolayers, and are terminated with ( $\text{TiO}_2$ ) or ( $\text{ZrO}_2$ ) monolayers. Then monolayer-by-monolayer epitaxial growth was modeled adding a pair of respective monolayers of BTO or PZO (001) symmetrically to both sides of a substrate slab until deposited BTO or PZO (001) thin films reach thickness of up to 10 monolayers (Fig. 1). In such a way we construct 10 heterostructures consisting of different thickness of deposited BTO and PZO nanofilms. Due to the restrictions imposed by the symmetry, in our simulations atomic positions of all atoms were relaxed only along the z axis, however the joint equilibrium lattice constant has been calculated for every interface under study. As the deposited thin film becomes thicker, the joint equilibrium lattice constant tends to expand toward its bulk value (BTO or PZO bulk), i.e. 1-layer thick BTO/STO interface possesses

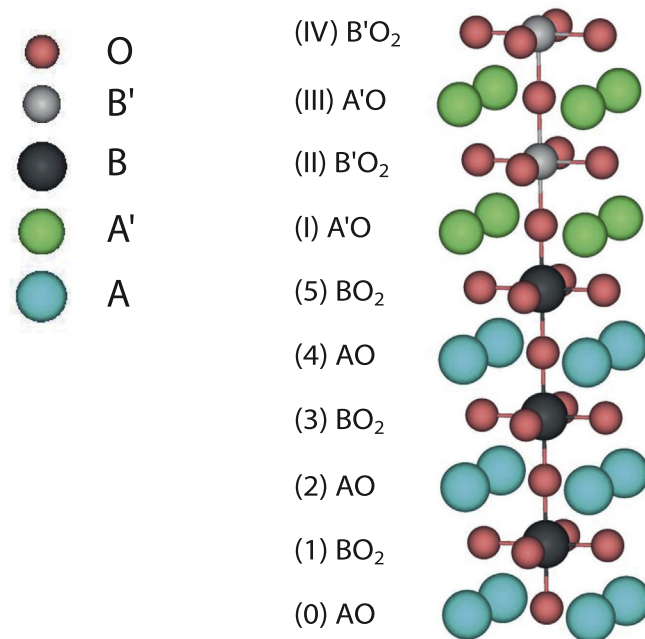


**Fig. 1.** Sketch of the (001) interface between the two wide band gap perovskites  $\text{ABO}_3$  and  $\text{A}'\text{B}'\text{O}_3$ . Planes of  $\text{A}'\text{B}'\text{O}_3$  (001) substrate are numbered with arabic numbers, while roman numbers are used to number planes of deposited  $\text{ABO}_3$  (001) film. Zero corresponds to the central plane on symmetrically terminated slab.

joint equilibrium lattice constant of  $3.925\text{ \AA}$  that is close to STO bulk value of  $3.902\text{ \AA}$  and 10-layer thick BTO/STO interface possesses joint equilibrium lattice constant of  $3.957\text{ \AA}$  that is closer to BTO bulk value of  $4.007\text{ \AA}$ ; 1-layer thick PZO/SZO interface possesses joint equilibrium lattice constant of  $4.164\text{ \AA}$  that is close to SZO bulk value of  $4.163\text{ \AA}$  and 10-layer thick PZO/SZO interface possesses joint equilibrium lattice constant of  $4.167\text{ \AA}$  that is close to PZO bulk value of  $4.177\text{ \AA}$ .

In order to analyze the electronic charge density redistribution we recognize what occurs in the electronic charge density in the heterostructures, compared to the isolated BTO and PZO, and STO and SZO (001) slab constituents. Charge density redistribution is defined as the electronic density in the heterointerface minus the sum of electron densities in separately isolated STO and SZO (001) substrate and BTO or PZO (001) thin film slabs, and is depicted in Fig. 2 for both 3- and 4-UC thick BTO/STO and PZO/SZO (001) interfaces. These plots show us that the most significant distortions occur at the interface due to the compensation of the surface effects of the slabs. They also show that the electronic structure of the substrate of non-stoichiometric heterostructures is distorted similarly to that of stoichiometric ones. The situation in the thin films is opposite. This fact well correlates with the predicted atomic structures.

Considering the density of states (DOS) projected layer by layer onto all orbitals of Ba, Sr, Pb, Ti, Zr, and O atoms of BTO/STO (001) and PZO/SZO (001) interfaces, as in case of bulk perovskites, the top of valence band is formed by O  $2p$  orbitals, while the bottom of the conduction band is formed mainly by Ti  $3d$  and Zr  $4d$  states. Ti–O and Zr–O hybridization are well pronounced. In case of BaO-terminated BTO/STO (001) and  $\text{ZrO}_2$ -terminated PZO/SZO (001) interfaces gained excess of electron density shifts occupied levels up that gives raise to the expanded band gap. In its turn, the PbO and  $\text{TiO}_2$ -terminated interfaces experiences the lack of electron density, that shifts occupied levels down and thus reduces the band gap of BTO/STO (001) and PZO/SZO (001) interfaces (Fig. 3).

**Table 1**

Equilibrium lattice constants ( $a_0$  in  $\text{\AA}$ ), atomic net charges ( $Q_{\text{atom}}$  in e), cation–O bond populations ( $P_{\text{A/B-O}}$  in milli e), and band gaps ( $\delta$  in eV) of bulk BTO, STO, SZO and PZO in their high-symmetry  $Pm\bar{3}m$  cubic phase are calculated by means of B3PW hybrid exchange–correlation functional within DFT. Negative bond population means atomic repulsion. Available experimental data are given in brackets. Band gaps listed here are indirect band gaps.

|                         | BTO                   | STO                    | PZO                    | SZO                    |
|-------------------------|-----------------------|------------------------|------------------------|------------------------|
| $a_0$                   | 4.007 (4.00)<br>[30]) | 3.903 (3.905)<br>[31]) | 4.177 (4.161)<br>[32]) | 4.163 (4.154)<br>[33]) |
| $Q_{\text{Ba/Sr/Pb}}$   | 1.79                  | 1.87                   | 1.30                   | 1.88                   |
| $Q_{\text{Ti/Zr}}$      | 2.36                  | 2.35                   | 2.07                   | 2.13                   |
| $Q_{\text{O}}$          | −1.39                 | −1.41                  | −1.12                  | −1.33                  |
| $P_{\text{Ba/Sr/Pb-O}}$ | −34                   | −10                    | 36                     | 0                      |
| $P_{\text{Ti/Zr-O}}$    | 100                   | 88                     | 100                    | 84                     |
| $P_{\text{O-O}}$        | −36                   | −44                    | −20                    | −8                     |
| $\delta$                | 3.50 (3.2)<br>[34])   | 3.63 (3.25)<br>[35])   | 3.79 (3.7<br>[36])     | 5.00 (5.6<br>[37])     |

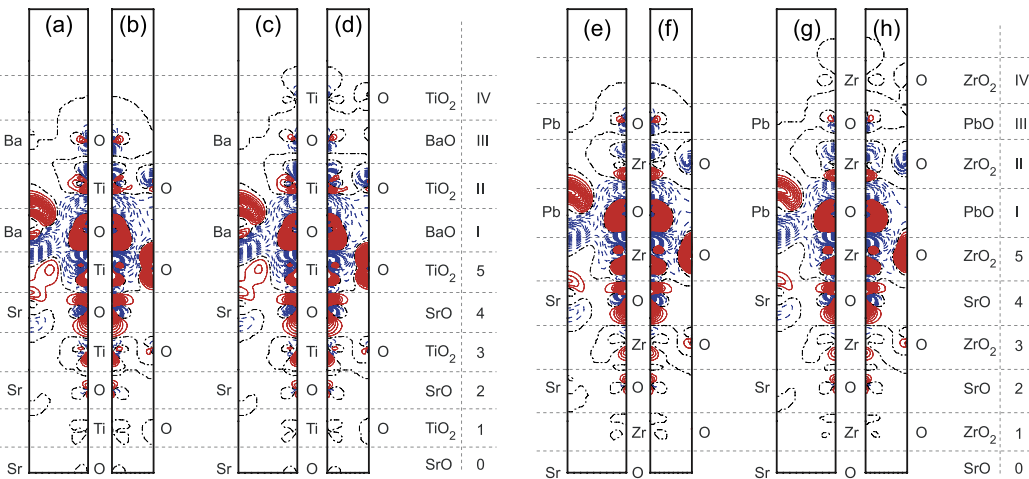


**Fig. 2.** Difference electron charge density maps calculated for BTO/STO (001) and PZO/SZO (001) heterostructures: (a) (110) cross-section for  $N_{\text{BTO}} = 3$ , (b) (100) cross-section for  $N_{\text{BTO}} = 3$ , (c) (110) cross-section for  $N_{\text{BTO}} = 4$ , (d) (100) cross-section for  $N_{\text{BTO}} = 4$  (e) (110) cross-section for  $N_{\text{PZO}} = 3$ , (f) (100) cross-section for  $N_{\text{PZO}} = 3$ , (g) (110) cross-section for  $N_{\text{PZO}} = 4$ , (h) (100) cross-section for  $N_{\text{PZO}} = 4$ . Red solid (dark gray), blue dashed (light gray) and black dash-dot isolines describe positive, negative and zero values of the difference charge density, respectively. Isodensity curves are drawn from  $-0.025$  to  $+0.025 \text{ e}^{-3}$  with an increment of  $0.0005 \text{ e}^{-3}$ . Right-side bar shows the atomic monolayers from which atoms are originated. Calculations are performed using B3PW hybrid exchange–correlation functional. STO and BTO monolayers are numbered beginning from the center of slab (0 means the central monolayer of the symmetrical slab unit cell). Monolayers (planes) are numbered separately for STO (001) and SZO (001) substrate and for BTO (001) and PZO (001) nanofilm with arabic and roman numbers, respectively. (For interpretation of the references to colour in this figure legend, the reader is referred to the web version of this article.)

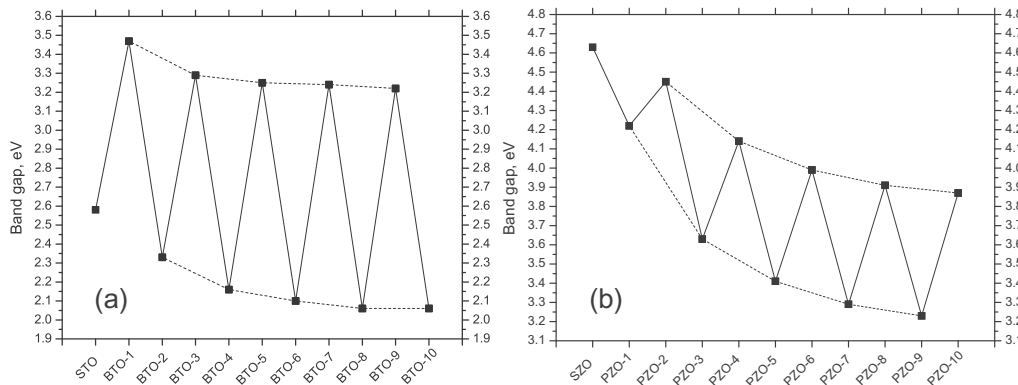


**Fig. 3.** Calculated optical band gaps of (a) BTO/STO (001) and (b) PZO/SZO (001) interfaces under study. Number of deposited BTO or PZO monolayers changes from zero ( $\text{TiO}_2$ - or  $\text{ZrO}_2$ -terminated STO or SZO substrate, respectively) to 10. Dashed lines are guide for eyes.

#### 4. Conclusions

We have performed *ab initio* calculations on a number of both stoichiometric and non-stoichiometric BTO/STO (001) and PZO/SZO (001) heterostructures. For both the BTO/STO (001) and PZO/SZO (001) interface the Ti–O and Zr–O chemical bond population is independent from the number of layers and larger than in the bulk. We find that the surface covalent effects in the non-stoichiometric films are less pronounced than in stoichiometric ones. All calculated BTO/STO and PZO/SZO (001) interfaces are semiconducting. In agreement with recent experimental study [15], we found that the interface layer do not influence much the electronic structure of studied structures, while termination of deposited BTO and PZO (001) thin film atop of STO or SZO (001) substrates may shift the band edges with respect to the vacuum level and thus reduce the band gap. From our point of view, such a prediction should be considered in further investigation of BTO/STO and PZO/SZO (001) heterostructures.

#### Acknowledgement

Authors thank Professor E.A. Kotomin for many fruitful discussions. This work has been supported by the Latvian Council of Science Grant No. 374/2012 and ESF Grant No. 2013/0046/1DP/1.1.1.2.0/13/APIA/VIAA/021.

#### References

- [1] R.I. Eglitis, D. Vanderbilt, First-principles calculations of atomic and electronic structure of  $\text{SrTiO}_3$  (001) and (011) surfaces, Phys. Rev. B 77 (2008) 195408, <http://dx.doi.org/10.1103/PhysRevB.77.195408>.
- [2] R.I. Eglitis, D. Vanderbilt, *Ab initio* calculations of  $\text{BaTiO}_3$  and  $\text{PbTiO}_3$  (001) and (011) surface structures, Phys. Rev. B 76 (2007) 155439, <http://dx.doi.org/10.1103/PhysRevB.76.155439>.
- [3] A. Höfer, M. Fechner, K. Duncker, M. Hölzer, I. Mertig, W. Widdra, Persistence of surface domain structures for a bulk ferroelectric above  $T_c$ , Phys. Rev. Lett. 108 (2012) 087602, <http://dx.doi.org/10.1103/PhysRevLett.108.087602>.
- [4] A.M. Kolpak, D. Li, R. Shao, A.M. Rappe, D.A. Bonnell, Evolution of the structure and thermodynamic stability of the  $\text{BaTiO}_3$  (001) surface, Phys. Rev. Lett. 101 (2008) 036102, <http://dx.doi.org/10.1103/PhysRevLett.101.036102>.

- [5] N. Erdman, K.R. Poeppelmeier, M. Asta, O. Warschkow, D.E. Ellis, L.D. Marks, The structure and chemistry of the  $TiO_2$ -rich surface of  $SrTiO_3$  (001), *Nature* 419 (2002) 55–58.
- [6] M. Dawber, K.M. Rabe, J.F. Scott, Physics of thin-film ferroelectric oxides, *Rev. Mod. Phys.* 77 (2005) 1083–1130, <http://dx.doi.org/10.1103/RevModPhys.77.1083>.
- [7] R.I. Eglitis, Ab initio calculations of  $SrTiO_3$ ,  $BaTiO_3$ ,  $PbTiO_3$ ,  $CaTiO_3$ ,  $SrZrO_3$ ,  $PbZrO_3$  and  $BaZrO_3$  (001), (011) and (111) surfaces as well as F centers, polarons, KTN solid solutions and Nb impurities therein, *Int. J. Mod. Phys. B* 28 (17) (2014) 1430009, <http://dx.doi.org/10.1142/S0217979214300096>.
- [8] E.A. Kotomin, R.I. Eglitis, J. Maier, E. Heifets, Calculations of the atomic and electronic structure for  $SrTiO_3$  perovskite thin films, *Thin Solid Films* 400 (1–2) (2001) 76–80, [http://dx.doi.org/10.1016/S0040-6090\(01\)01454-7](http://dx.doi.org/10.1016/S0040-6090(01)01454-7). Proceedings of Symposium N on Ultrathin Oxides.
- [9] J. Dionot, G. Geneste, C. Mathieu, N. Barrett, Surface polarization, rumpling, and domain ordering of strained ultrathin  $BaTiO_3$  (001) films with in-plane and out-of-plane polarization, *Phys. Rev. B* 90 (2014) 014107, <http://dx.doi.org/10.1103/PhysRevB.90.014107>.
- [10] Y. Kim, R.M. Lutchyn, C. Nayak, Origin and transport signatures of spin-orbit interactions in one- and two-dimensional  $SrTiO_3$ -based heterostructures, *Phys. Rev. B* 87 (2013) 245121, <http://dx.doi.org/10.1103/PhysRevB.87.245121>.
- [11] Z. Zhong, A. Tóth, K. Held, Theory of spin-orbit coupling at  $LaAlO_3/SrTiO_3$  interfaces and  $SrTiO_3$  surfaces, *Phys. Rev. B* 87 (2013) 161102, <http://dx.doi.org/10.1103/PhysRevB.87.161102>.
- [12] R.I. Eglitis, G. Borstel, E. Heifets, S. Piskunov, E.A. Kotomin, Ab initio calculations of the  $BaTiO_3$  (100) and (110) surfaces, *J. Electroceram.* 16 (2006) 289–292.
- [13] R.I. Eglitis, M. Rohlffing, First-principles calculations of the atomic and electronic structure of  $SrZrO_3$  and  $PbZrO_3$  (001) and (011) surfaces, *J. Phys. Cond. Matter* 22 (41) (2010) 415901. <http://stacks.iop.org/0953-8984/22/i=41/a=415901>.
- [14] V. Stepkova, P. Marton, N. Setter, J. Hlinka, Closed-circuit domain quadruplets in  $BaTiO_3$  nanorods embedded in a  $SrTiO_3$  film, *Phys. Rev. B* 89 (2014) 060101, <http://dx.doi.org/10.1103/PhysRevB.89.060101>.
- [15] Z. Bi, B.P. Uberuaga, L.J. Vernon, E. Fu, Y. Wang, N. Li, H. Wang, A. Misra, Q.X. Jia, Radiation damage in heteroepitaxial  $BaTiO_3$  thin films on  $SrTiO_3$  under Ne ion irradiation, *J. Appl. Phys.* 113 (2) (2013), <http://dx.doi.org/10.1063/1.4775495>.
- [16] A.I. Lebedev, Band offsets in heterojunctions formed by oxides with cubic perovskite structure, *Phys. Solid State* 56 (5) (2014) 1039–1047, <http://dx.doi.org/10.1134/S106378341405014X>.
- [17] A.I. Lebedev, Ground state and properties of ferroelectric superlattices based on crystals of the perovskite family, *Phys. Solid State* 52 (7) (2010) 1448–1462, <http://dx.doi.org/10.1134/S1063783410070218>.
- [18] S. Piskunov, R.I. Eglitis, First principles hybrid DFT calculations of  $BaTiO_3/SrTiO_3$  (001) interface, *Solid State Ionics* 274 (2015) 29–33, <http://dx.doi.org/10.1016/j.ssi.2015.02.020>. URL: <<http://www.sciencedirect.com/science/article/pii/S0167273815000673>>.
- [19] K.D. Fredrickson, A.A. Demkov, Switchable conductivity at the ferroelectric interface: nonpolar oxides, *Phys. Rev. B* 91 (2015) 115126, <http://dx.doi.org/10.1103/PhysRevB.91.115126>.
- [20] N. Al-Aqtash, A. Alsaad, R. Sabirianov, Ferroelectric properties of  $BaZrO_3/PbZrO_3$  and  $SrZrO_3/PbZrO_3$  superlattices: an ab-initio study, *J. Appl. Phys.* 116 (7) (2014), <http://dx.doi.org/10.1063/1.4893300>.
- [21] A.D. Becke, Density-functional thermochemistry. III. The role of exact exchange, *J. Chem. Phys.* 98 (1993) 5648–5652.
- [22] E.A. Kotomin, S. Piskunov, Y.F. Zhukovskii, R.I. Eglitis, A. Gopeyenko, D.E. Ellis, The electronic properties of an oxygen vacancy at  $ZrO_2$ -terminated (001) surfaces of cubic  $PbZrO_3$ : computer simulation from the first principles, *Phys. Chem. Chem. Phys.* 10 (2008) 4258–4263.
- [23] S. Piskunov, A. Gopeyenko, E.A. Kotomin, Y.F. Zhukovskii, D.E. Ellis, Atomic and electronic structure of perfect and defective  $PbZrO_3$  perovskite: hybrid DFT calculations of cubic and orthorhombic phases, *Comput. Mater. Sci.* 41 (2007) 195–201.
- [24] R. Dovei, V.R. Saunders, C. Roetti, R. Orlando, C.M. Zicovich-Wilson, F. Pascale, B. Civalleri, K. Doll, N.M. Harrison, I.J. Bush, Ph. D'Arco, M. Llunell, CRYSTAL09 User's Manual, University of Torino, Torino, 2009. <<http://www.crystal.unito.it/>>.
- [25] S. Piskunov, E. Heifets, R.I. Eglitis, G. Borstel, Bulk properties and electronic structure of  $SrTiO_3$ ,  $BaTiO_3$ ,  $PbTiO_3$  perovskites: an ab initio HF/DFT study, *Comput. Mater. Sci.* 29 (2004) 165–178.
- [26] P.J. Hay, W.R. Wadt, Ab initio effective core potentials for molecular calculations. Potentials for K to Au including the outermost core orbitals, *J. Chem. Phys.* 82 (1) (1984) 299–310.
- [27] S. Piskunov, E. Spohr, T. Jacob, E.A. Kotomin, D.E. Ellis, Electronic and magnetic structure of  $La_{0.875}Sr_{0.125}MnO_3$  calculated by means of hybrid density-functional theory, *Phys. Rev. B* 76 (2007) 012410.
- [28] R.S. Mulliken, Electronic population analysis on LCAO-MO molecular wave functions, *J. Chem. Phys.* 23 (12) (1955) 1833, 1841, 2338, 2343.
- [29] H.J. Monkhorst, J.D. Pack, Special points for Brillouin-zone integrations, *Phys. Rev. B* 13 (12) (1976) 5188–5192.
- [30] K.H. Hellwege, A.M. Hellwege (Eds.), *Ferroelectrics and Related Substances*, New Series, Landolt-Bornstein, Springer Verlag, Berlin, group III, vol. 3, 1969.
- [31] Y.A. Abramov, V.G. Tsirelson, V.E. Zavodnik, S.A. Ivanov, I.D. Brown, The chemical bond and atomic displacements in  $SrTiO_3$  from X-ray diffraction analysis, *Acta Cryst. B* 51 (1995) 942–951.
- [32] S. Aoyagi, Y. Kuroiwa, A. Sawada, H. Tanaka, J. Harada, E. Nishibori, M. Takata, M. Sakata, Direct observation of covalency between O and disordered Pb in cubic  $PbZrO_3$ , *J. Phys. Soc. Jpn.* 71 (10) (2002) 2353–2356.
- [33] B.J. Kennedy, C.J. Howard, B.C. Chakoumakos, High-temperature phase transitions in  $SrZrO_3$ , *Phys. Rev. B* 59 (1999) 4023–4027, <http://dx.doi.org/10.1103/PhysRevB.59.4023>.
- [34] S.H. Wemple, Polarization fluctuations and the optical-absorption edge in  $BaTiO_3$ , *Phys. Rev. B* 2 (7) (1970) 2679–2689.
- [35] K. van Benthem, C. Elsässer, R.H. French, Bulk electronic structure of  $SrTiO_3$ : experiment and theory, *J. Appl. Phys.* 90 (12) (2001) 6156–6164.
- [36] J. Robertson, Band offsets of wide-band-gap oxides and implications for future electronic devices, *J. Vac. Sci. Technol. B* 18 (3) (2000) 1785–1791.
- [37] Y.S. Lee, J.S. Lee, T.W. Noh, D.Y. Byun, K.S. Yoo, K. Yamaura, E. Takayama-Muromachi, Systematic trends in the electronic structure parameters of the 4d transition-metal oxides  $SrMO_3$  ( $M = Zr, Mo, Ru, and Rh$ ), *Phys. Rev. B* 67 (2003) 113101, <http://dx.doi.org/10.1103/PhysRevB.67.113101>.